

1 **ABSTRACT**

2 Atomically thin cuprates exhibiting a superconducting phase transition temperature similar to bulk have
3 recently been realized, although the device fabrication remains a challenge and limits the potential for
4 many novel studies and applications. Here we use an optical pump-probe approach to noninvasively study
5 the unconventional superconductivity in atomically thin $\text{Bi}_2\text{Sr}_2\text{Ca}_{0.92}\text{Y}_{0.08}\text{Cu}_2\text{O}_{8+\delta}$ (Y-Bi2212). Apart from
6 finding an optical response due to the superconducting phase transition that is similar to bulk Y-Bi2212,
7 we observe that the sign and amplitude of the pump-probe signal in the atomically thin flake vary
8 significantly in different dielectric environments depending on the nature of the optical excitation. By
9 exploiting the spatial resolution of the optical probe, we uncover the exceptional sensitivity of monolayer
10 Y-Bi2212 to the environment. Our results provide the first optical evidence for the intralayer nature of the
11 superconducting condensate in Bi2212, and highlight the role of double-sided encapsulation in preserving
12 superconductivity in atomically thin cuprates.

13
14 **KEYWORDS:** 2D materials, cuprate, high- T_c superconductivity, optical pump-probe
15 spectroscopy

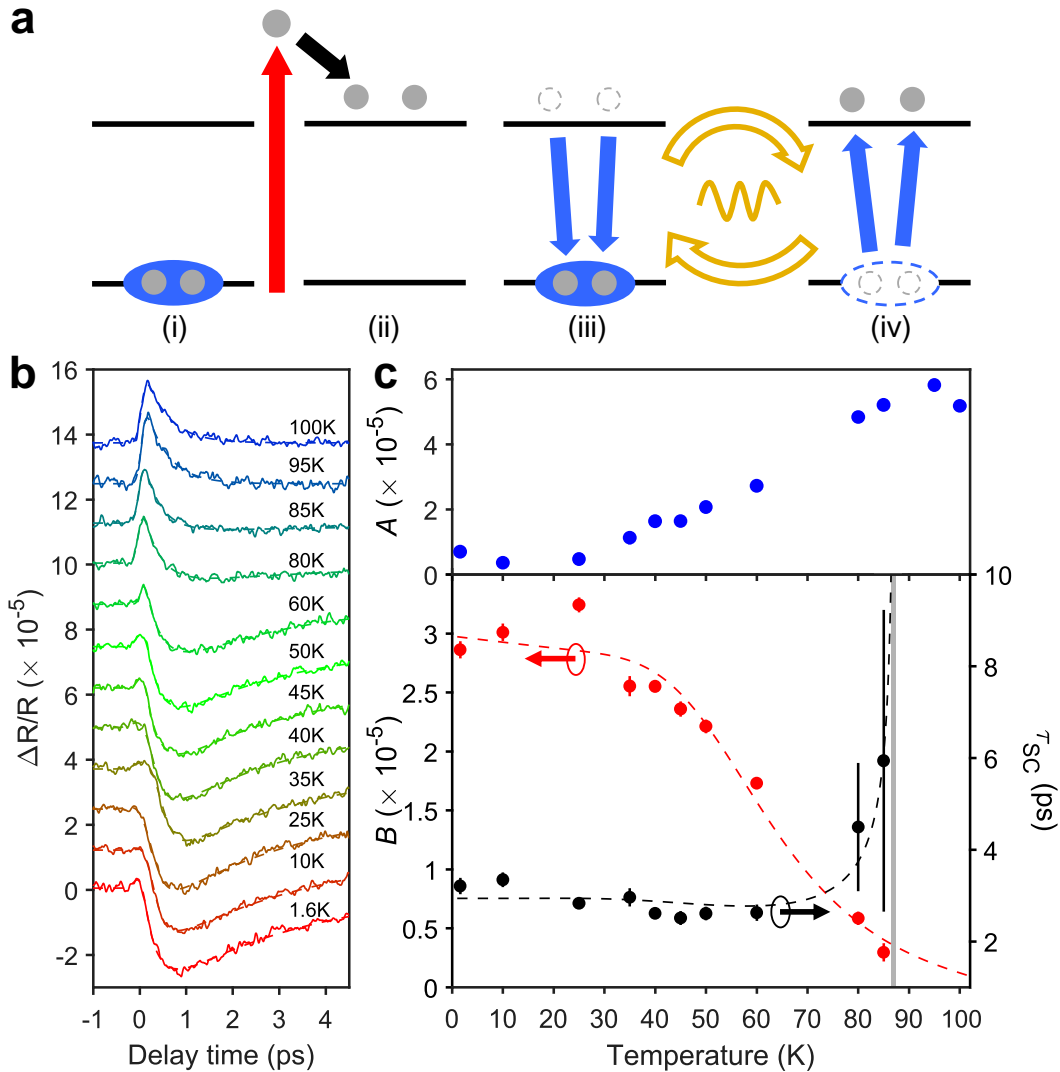
1 The successful isolation of monolayer (ML) $\text{Bi}_2\text{Sr}_2\text{CaCu}_2\text{O}_{8+\delta}$ (Bi2212) has opened up many
2 exciting possibilities for studying two-dimensional (2D) superconductivity and fabricating novel
3 devices using atomically thin high- T_c superconductors (2D-HTSCs)¹. Recent experiments have
4 revealed that novel phenomena such as the interfacial Josephson effect and superconducting
5 diode effect can emerge in artificially twisted Bi2212 stacks²⁻⁵. Theoretically, it has been
6 predicted that such twisted stacks can host more exotic physics, including topological
7 superconductivity with broken time-reversal symmetry⁶⁻⁸. However, fabricating high-quality
8 cuprate devices and probing their intrinsic properties through transport measurements remains a
9 challenging task. One of the primary challenges lies in the susceptibility of atomically thin
10 Bi2212 to degradation during conventional nanofabrication processes due to oxygen dopant loss
11 and reaction with moisture^{1,9-11}. To mitigate these issues, stencil mask lithography and limited-
12 heating evaporation have been employed to reduce the damage of electrical contact fabrication in
13 relatively thick flakes^{10,12}. Additionally, a cold welding approach has been developed to preserve
14 the ML sample quality¹, although this method requires implementing a series of intricate
15 processes in a stringent environment. In this study, we propose an alternative approach to
16 investigate the superconductivity in atomically thin Bi2212 using ultrafast optical pump-probe
17 spectroscopy, a noninvasive probe with micron-sized spatial resolution that allows us to study
18 the interaction of 2D-HTSCs with different local environments.

19 Ultrafast optical pump-probe spectroscopy has been successfully applied to study
20 superconductivity in bulk HTSCs¹³. In these measurements, an ultrafast pump pulse is firstly
21 applied to samples of over 100-nm thickness to break the Cooper pairs. The transiently formed
22 non-equilibrium quasiparticles alter the optical conductivity and reflectivity, which is measured
23 with an ultrashort probe pulse with a variable time delay following the pump pulse. Remarkably,

1 the superconducting phase transition can be observed by monitoring the decay time constant τ of
2 the transient reflection signal. In the superconducting phase, τ is several times longer than at
3 temperatures above T_c . This contrast has been understood as a phonon bottleneck effect in
4 superconductors^{14,15}, where photoexcited quasiparticles quickly relax to the superconducting gap
5 edge and recombine while emitting numerous gap-frequency phonons (GFPs) (Figure 1a). These
6 GFPs can further break other Cooper pairs, re-excite the quasiparticles, and generate new GFPs,
7 until the energy dissipates through anharmonic decay^{13,16}. As a result, τ is usually a few
8 picoseconds long in the superconducting phase and is often associated with the GFP decay time.
9 In contrast, such a bottleneck effect is absent in the non-superconducting phase, where τ becomes
10 shorter than 1 ps^{17,18}. Although the phonon bottleneck equations are derived for the isotropic *s*-
11 wave superconducting gap, the photoexcitation and relaxation of quasiparticles in *d*-wave
12 cuprates are expected to take place mainly at antinodes^{16,19-21}, where the gap size is maximized
13 and used in the phonon bottleneck effect.

14 In this work, we push the limit of this optical sensing technique and apply it to atomically thin
15 Y-Bi2212. We find that the majority of the bulk behaviors persist in the atomically thin limit.
16 Specifically, we find a similar change of the decay time constant τ near the phase transition and
17 the ability of a strong pump pulse to induce a non-superconducting phase below T_c . These
18 agreements with the bulk observations elucidate the 2D nature of Cooper pairs in Bi2212²²⁻²⁸,
19 where the superconductivity is predominantly hosted by two coupled CuO₂ planes. On the other
20 hand, we find atomically thin Y-Bi2212 to be easily affected by the local environment. Enabled
21 by the spatial resolution offered by our optical technique, we are able to resolve the transient
22 reflection signal in different local environments, which allows us to resolve the complex
23 permittivity contrast in the superconducting and non-superconducting components of the pump-

1 probe signal. In addition, we find that a suspended Y-Bi2212 monolayer can be extremely
 2 sensitive to the residual gas through either the upper or lower exposed surface, and a double-
 3 sided encapsulation proves effective in preserving the superconductivity.
 4



5
 6
 7 **Figure 1.** (a) The phonon bottleneck effect involved in the relaxation of optical excitations in
 8 high- T_c superconductors. (i) Photoexcitation (red arrow) breaks Cooper pairs and generates
 9 quasiparticles above the superconducting gap. (ii) Thermalization occurs as quasiparticles relax
 10 to the states near the edges of the superconducting gap. (iii) Quasiparticles can recombine into
 11 Cooper pairs only by emitting phonons with the gap energy. (iv) The gap frequency phonon

1 (GFP) breaks another Cooper pair and brings the system back to the condition of (iii). The
2 cyclical process between (iii) and (iv) continues until GFPs decay through the anharmonic
3 processes or diffuse out of the probing spot. (b) Temperature dependence of the pump-probe
4 response of a four-layer (4L) Y-Bi2212 flake measured at a pump fluence of $44.5 \mu\text{J}/\text{cm}^2$. Curves
5 for $T > 1.6 \text{ K}$ are shifted vertically. Dashed lines are the fit results based on a single exponential
6 (for 1.6 K, 95 K and 100 K) or a bi-exponential function (for all other temperatures). (c) Top
7 panel: extracted PG component amplitude A (blue circles) at each temperature. The PG
8 component emerges near 40K and becomes larger with increasing temperature. Bottom panel:
9 extracted SC component amplitude B (red circles) and decay time constant τ_{SC} (black circles) at
10 each temperature. The uncertainty in τ_{SC} becomes very large near T_c as the SC component
11 vanishes near the phase transition. Fitted curves are shown by dashed lines. The gray vertical bar
12 highlights the T_c from τ_{SC} fitting from the signals of the 4L sample.

13
14 We start by measuring the temperature dependence of the pump-probe response in a four-layer
15 (4L) sample. Following the convention in the field, each monolayer is defined as half of the
16 Bi2212 unit cell and contains two CuO_2 planes separated by a Ca plane^{1,29} (Figure S1). We use
17 ~ 100 -fs pump (1200 nm) and probe (800 nm) pulses for our optical pump-probe experiments.
18 Details about the experimental methods can be found in the Supporting Information. We first
19 identify the characteristics of the time-resolved signals at temperatures both below and above the
20 bulk crystal T_c with a pump fluence of $44.5 \mu\text{J}/\text{cm}^2$. At base temperature (1.6 K), the pump
21 reduces the transient reflection of the probe. The negative signal initially rises in ~ 100 fs and
22 then gradually recovers over a few ps. At 100 K, the pump-probe signal is positive and the decay
23 occurs mostly within one ps (Figure 1b). To quantify this contrast, a single exponential decay

1 convoluted with a Gaussian pump pulse shape function is used to extract the respective time
2 constants. The time constant τ of the slow recovery at 1.6 K is about 3.2 ps, eight times slower
3 than the fast decay at 100 K (~ 0.4 ps). These observations agree with the so-called
4 superconducting (SC) and pseudogap (PG) components in bulk HTSCs, where the values of the
5 time constant are $\tau_{SC} \approx 2.5$ ps and $\tau_{PG} \approx 0.5$ ps respectively¹⁷, suggesting that superconductivity is
6 preserved and the phonon bottleneck effect persists in atomically thin Bi2212. We further
7 confirm the strong correlation between the slow-decaying pump-probe signal and
8 superconductivity by carrying out optical and electrical four-probe resistance measurements in
9 the same 10-layer sample. Detailed information is available in the Supporting Information.

10 The results at intermediate temperatures are more complicated as they involve both positive
11 and negative components due to the pump-induced phase transition of some regions from the SC
12 phase to the PG phase. We fit these signals with the combination of two exponential decays³⁰,
13 $Ae^{-t/\tau_{PG}} - Be^{-t/\tau_{SC}}$, where A (B) and τ_{PG} (τ_{SC}) are the amplitude and time constant of the PG
14 (SC) component, respectively, and the result of this analysis is shown in Figure 1c. As
15 temperature increases, the amplitude of the SC component diminishes and falls below the
16 detection limit at 95 K and 100 K. Assuming that B is proportional to the photoexcited Cooper
17 pair density, we can fit $B(T)$ with a two-temperature model previously developed for bulk
18 HTSCs¹⁶. On the other hand, τ_{SC} increases with increasing temperature near T_c , which can be
19 understood in terms of the Ginzburg-Landau theory of second-order phase transitions³¹. As the
20 temperature approaches T_c , the restoring force corresponding to the derivative of the system's
21 free energy with respect to the SC order parameter diminishes, and therefore the relaxation to
22 equilibrium after a sudden pump becomes infinitely long. The seeming divergent behavior of τ_{SC}
23 agrees with previous pump-probe studies of bulk HTSCs^{16,17,30,32}. By fitting the τ_{SC} with the

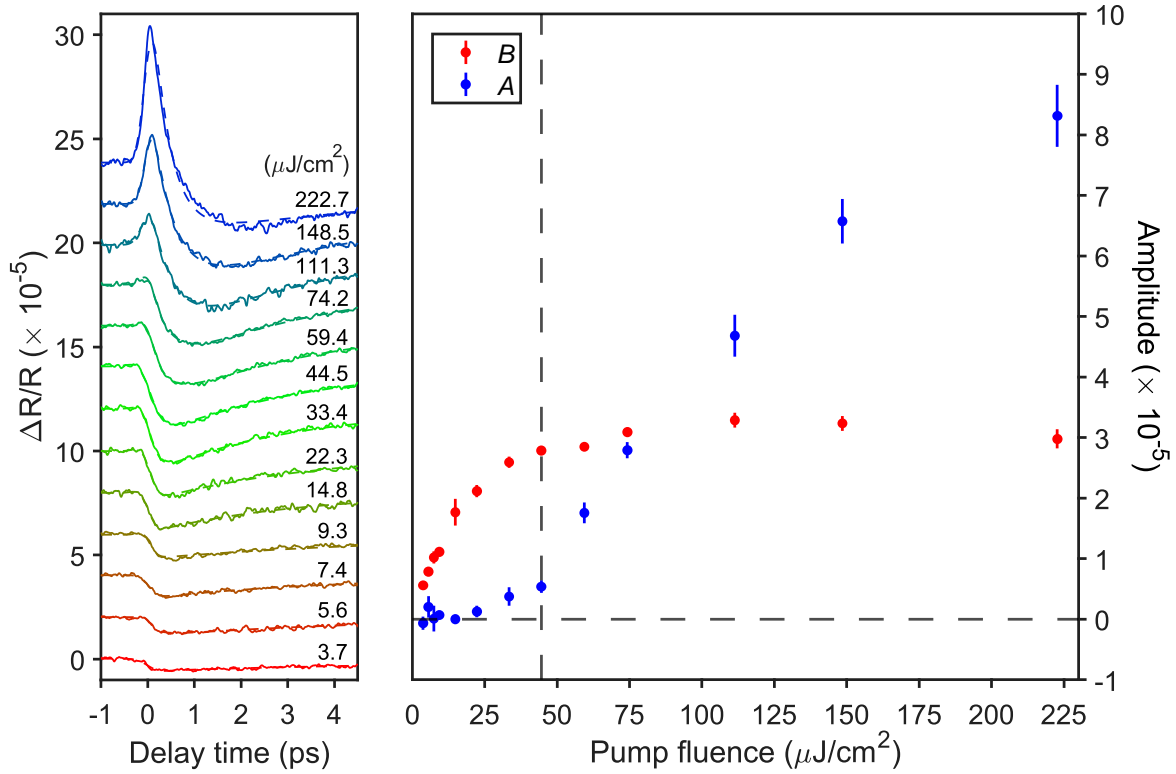
1 phonon decay lifetime in the superconducting state¹⁶, we acquire a T_c of ~ 87 K. The bulk T_c of \sim
2 92 K (slightly underdoped Y-Bi2212) falls within the uncertainty of our measured T_c (see
3 Supporting Information for details). The similar overall temperature dependence and
4 superconducting transition temperature confirm that the SC gap in Bi2212 is not affected by the
5 reduced dimension.

6 The existence of both SC and PG components at intermediate temperatures can be explained
7 by a photoinduced phase transition (PIPT) triggered by a pump pulse above a certain threshold
8 fluence (Φ_{th})^{18,30,33–36}. At low pump fluence, only a small number of Cooper pairs become
9 quasiparticles and their relaxation is governed by the phonon bottleneck effect. When Cooper
10 pairs are pumped strongly with a fluence exceeding the threshold, in our case $\Phi_{th} \approx 50 \mu\text{J}/\text{cm}^2$ at
11 1.6 K, some regions of the material go through a phase transition and enter the pseudogap
12 phase³⁴. Such a transient phase was previously attributed to a collection of Cooper pairs without
13 phase coherence²⁵ and argued to be non-thermal^{18,30}. An alternative explanation for the
14 coexistence of both components is a percolation model, which considers a broad distribution of
15 gaps and nanoscale superconducting patches that proliferate in the material upon cooling^{37,38}, and
16 increased fluence may convert the patches into non-superconducting ones. This description was
17 introduced also in relation to the overall superconducting phenomenology of cuprates and oxide
18 superconductors³⁹.

19 The pump-induced mixed phase can be clearly seen in our 4L sample even at 1.6 K (Figure 2a).
20 As the pump fluence increases, the dynamics gradually changes from a single-exponential
21 recovery to a double-exponential decay at intermediate temperatures. When the fluence is small,
22 the fitted amplitude B increases linearly with the fluence and the amplitude A is negligible
23 (Figure 2b). Above $\Phi_{th} \approx 50 \mu\text{J}/\text{cm}^2$, the strong pump saturates the SC component while the PG

1 component appears and dominates the signal in the first few hundreds of femtoseconds. Our
2 reported temperature dependence in Figure 1b is measured with a pump fluence of $44.5 \mu\text{J}/\text{cm}^2$,
3 as indicated by the vertical dashed line, which is close to Φ_{th} . Nevertheless, the SC gap decreases
4 as the temperature increases, which reduces Φ_{th} . Consequently, the intermediate temperature
5 dependence results reported in Figure 1b are likely in the early saturation regime, which leads to
6 the observed PG component. This saturation may also slightly distort the fitted amplitude of the
7 SC component, but the time constant and the retrieved T_c should not be influenced, because the
8 decay time constant may only be affected by the fluence at the lowest temperature due to a
9 possible two-particle kinetics^{15,18,40}, while the saturation occurs at higher temperatures.

10 Interestingly, the observed low-temperature saturation threshold ($\sim 50 \mu\text{J}/\text{cm}^2$) is comparable to
11 that in bulk Bi2212, where the collapse of superconductivity has been reported for pump
12 fluences ranging from $14 \mu\text{J}/\text{cm}^2$ to $70 \mu\text{J}/\text{cm}^2$ ^{213,30,33–36}. Given the dielectric functions of Y-
13 Bi2212⁴¹, SiO₂ (285 nm), and hBN (15 nm), we calculate and find that the average absorption
14 per layer at 1200 nm (pump wavelength) in both bulk and the 4L Y-Bi2212 are similar.
15 Therefore, we conclude that the intrinsic PIPT threshold fluence is not changed in the atomically
16 thin Bi2212, implying that the phase coherence of the SC condensate is not related to the
17 coupling between layers.



1
2 **Figure 2.** (a) Fluence dependence of the pump-probe response of the 4L Y-Bi2212 sample at 1.6
3 K. (b) Extracted PG and SC component amplitudes, labeled by A (blue circles) and B (red circles)
4 respectively. The vertical dashed line indicates the fluence (44.5 $\mu\text{J}/\text{cm}^2$) applied for the
5 temperature dependence measurement (Figure 1b).

6

7 So far, we have demonstrated that the atomically thin Bi2212 manifests many similar optical
8 properties as the bulk. In addition to the above findings, we have discovered novel properties that
9 arise from the atomically thin nature of 2D-HTSC. Specifically, we find that the pump-probe
10 response of a thin flake can be significantly modified by the environment. This environmental
11 contrast provides us with the ability to resolve the complex permittivity change associated with
12 different optical excitations.

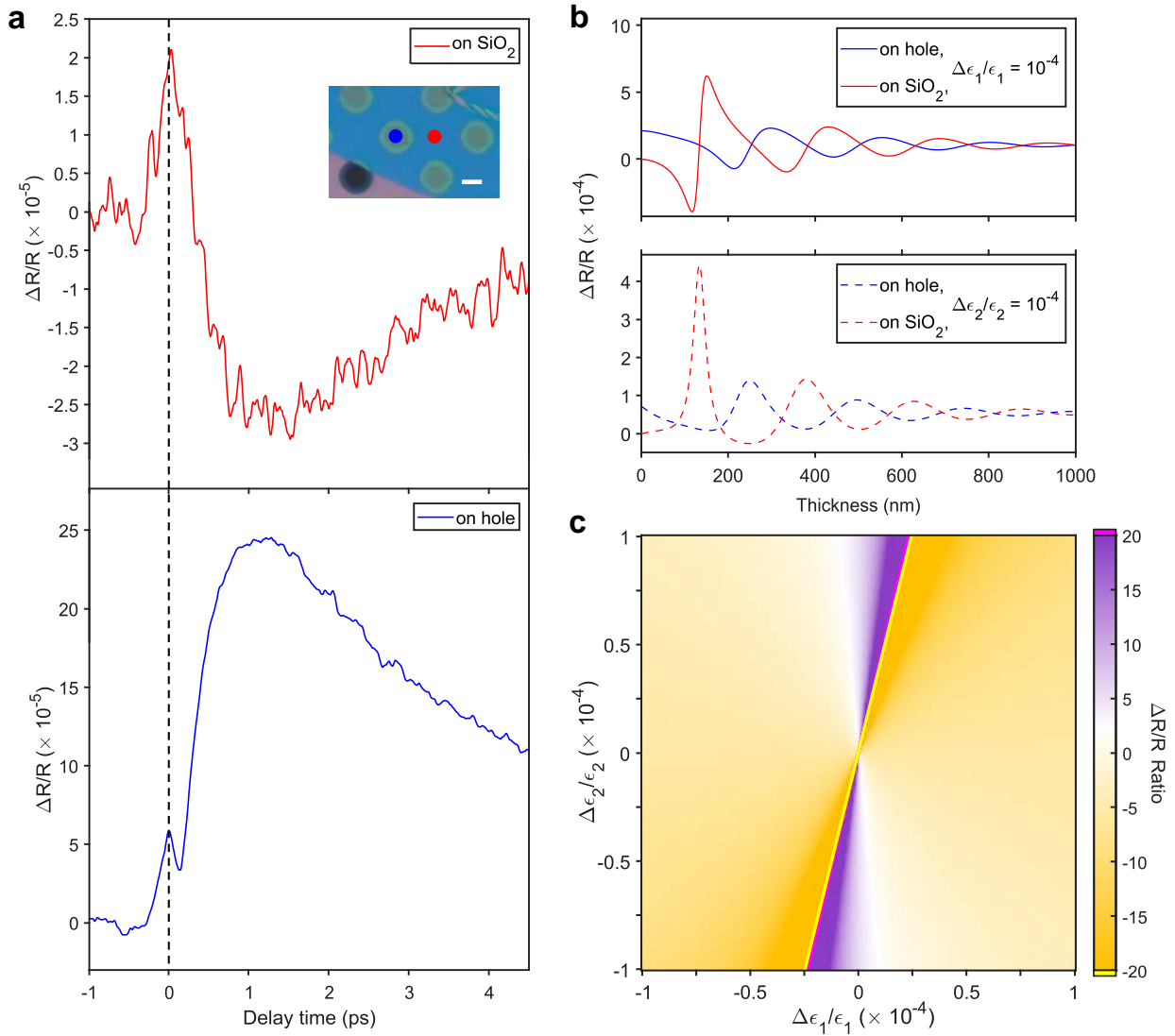
1 To this end, we conduct experiments on flakes prepared on substrates prepatterned with hole
2 arrays. The SiO₂ substrate and holes provide large permittivity contrast at the optical frequency,
3 which allows us to measure different pump-probe responses at 1.6 K. To avoid complications
4 due to the hBN encapsulation layer, we use a relatively thick Y-Bi2212 flake (40 nm), which is
5 more robust to oxygen dopant loss, but still thinner than the optical skin depth⁴² (~ 100 nm). In
6 the area supported by the substrate, we observe a response similar to that of the 4L flake: with a
7 strong pump above the threshold fluence, the signal shows a slow SC component with a negative
8 sign and a fast PG component with a positive sign (top panel in Figure 3a). Interestingly, in the
9 suspended area, the slow SC component turns positive, and its amplitude becomes more than ten
10 times stronger, while the fast PG component remains positive with an about three times stronger
11 amplitude (bottom panel in Figure 3a). Since the two probe spots are only a few micrometers
12 apart, this sign change is unlikely due to the local oxygen doping level difference between these
13 two sample areas, in contrast to the case for bulk samples where the doping level usually
14 determines the sign change behavior^{41,43}.

15 Through a series of calculations based on the transfer-matrix formalism, we conclude that the
16 contrast stems from the nature of the optical excitations. We simulate the sign and amplitude of
17 the pump-probe response using the transfer-matrix method based on each layer's dielectric
18 function and dimension. The pump-induced optical conductivity change of the sample is
19 modeled as a relatively small permittivity change ($\leq 10^{-4}$), either in the real (ϵ_1) or imaginary (ϵ_2)
20 part of the sample layer, while other layers are unaffected by the pump. To compare with the
21 experiment, we normalize the reflectivity change of the probe beam between the pump on and
22 off conditions to the absolute reflectivity. As the calculation result in Figure 3b shows, the sign
23 and amplitude of $\Delta R / R$ are significantly affected by an interference effect. In all scenarios, $\Delta R /$

1 R oscillates with the film thickens, with a periodicity matching the half- λ condition for the probe
2 light in Bi2212. For a flake of a certain thickness, the sign of $\Delta R / R$ is dependent on the nature
3 of the permittivity change and local dielectric environment. In the thick limit ($> 1\mu\text{m}$), the probe
4 beam can barely penetrate through the Bi2212 layer, resulting in a vanishing interference effect
5 and a convergence to the bulk limit.

6 The calculated $\Delta R / R$ contrast between the supported and suspended area is summarized in a
7 ratio plot (Figure 3c). When the pump-induced complex permittivity change is dominated by the
8 imaginary part ($\Delta\epsilon_1 / \epsilon_1$ close to zero), $\Delta R / R$ exhibits the same sign in both areas, mirroring the
9 behavior of the fast PG component. Under other conditions, $\Delta R / R$ changes its sign, similar to
10 the behavior of the slow SC component. These correspondences are supported by a
11 phenomenological model developed to describe the dielectric response of Y-Bi2212⁴¹.
12 According to this model, the PG component is attributed to a pump-induced broadening of the
13 Drude peak so that mainly the ϵ_2 contribution is transiently modified. On the other hand, the SC
14 component stems from the pump-induced changes in the Lorentzian oscillator of the interband
15 transition at 1.5 eV, leading to changes in both ϵ_1 and ϵ_2 . Our probe light measures a different
16 combination of ϵ_1 and ϵ_2 in the supported area and the suspended area. As a result, the PG
17 component (with mainly changes in ϵ_2) is associated with enhancement in the transient
18 reflectivity in both areas, while the SC component (with changes in both ϵ_1 and ϵ_2) induces
19 opposite $\Delta R / R$ changes between the two areas. The unique contrast in the permittivity change
20 between the PG and the SC components is interpreted as an indication of an unconventional
21 superconductivity-induced carrier kinetic energy loss⁴¹.

22



1
2 **Figure 3.** (a) The pump-probe response of a suspended Y-Bi2212 sample showing a large
3 contrast compared to the area supported by SiO_2 . The measured spots in the suspended and
4 supported areas are indicated by blue and red dots in the optical microscope image (inset),
5 respectively. The scale bar is $5 \mu\text{m}$. The supported area shows a positive fast and a negative slow
6 component, while both the fast and slow responses in the suspended area are positive. The
7 vertical dashed line is the zero time delay. (b) The calculated flake thickness dependence of
8 normalized transient reflectivity from the suspended (blue) and supported (red) areas. The top
9 panel shows the contrast when the permittivity change is real, and the bottom panel corresponds

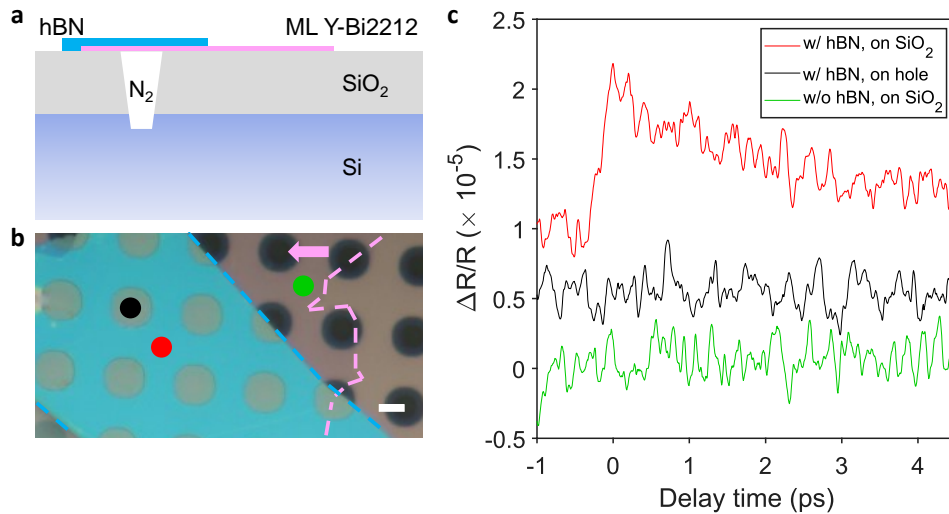
1 to a purely imaginary permittivity change. (c) Calculated ratio of transient reflectivity of the
2 suspended and supported areas for a 40-nm thick Y-Bi2212 flake. The purple and gold areas
3 represent the sign-conserving and sign-reversing conditions, respectively.

4
5 In the second example, we push the thickness limit and apply the pump-probe technique to a
6 monolayer (ML) Y-Bi2212 flake prepared on a prepatterned substrate (Figure 4a). In Figure 4b,
7 the area left to the pink dashed line contains a ML, half of which is covered by hBN, which
8 appears blue in the optical microscope image. The pump-probe responses of three representative
9 spots are measured at 1.6 K with a μm -level spatial resolution, as illustrated in Figure 4c. Clearly,
10 only the ML sandwiched between hBN and SiO_2 (red dot) remains superconducting, showing a
11 slow-decaying dynamics similar as the SC component in thicker flakes. A fluence of $74 \mu\text{J}/\text{cm}^2$
12 is utilized here to achieve a sufficient signal-to-noise ratio on the ML, thus both SC and PG
13 components are observed. The signs of both components are positive, potentially due to the local
14 dielectric environment of the sample. The SC component persists up to ~ 60 K, which we
15 identify as the T_c of the ML sample.

16 In contrast to the red-dotted position, the sample at the other two locations shows no response
17 above the noise floor at base temperature, indicating a complete quench of the superconductivity,
18 which cannot result from the dielectric environment difference according to our transfer matrix
19 calculations. We expect the null signals to have the following two potential causes: (i) The
20 sample becomes amorphous after reacting with the residual water vapor in a gaseous
21 environment¹⁰; (ii) The sample becomes insulating as the oxygen dopant leaves over time at
22 room temperature^{1,11}. Both conditions are equally possible for the exposed area (green dot),
23 because the sample without hBN coverage is directly in contact with the ambient environment

1 before being loaded into the cryostat. For the hBN-covered suspended area (black dot), the
 2 oxygen dopant loss is more likely a reason for the loss of superconductivity since the N₂ trapped
 3 in the hole should contain little moisture or oxygen from the glovebox. Both results indicate that
 4 monolayer Y-Bi2212 is extremely sensitive to the environment, and it is crucial to encapsulate
 5 them from both sides. In our experiment, hBN and SiO₂ provide effective barriers for hampering
 6 the migration of water vapor and oxygen dopants. A similar protection has also been
 7 demonstrated using graphene⁹.

8



9

10 **Figure 4.** (a) Schematic of a ML Y-Bi2212 sample prepared on a prepatterned substrate. A piece
 11 of hBN (blue) covers the ML Y-Bi2212 sample (pink) as an overlayer. (b) Corresponding optical
 12 microscope image. Dashed lines outline the boundaries for hBN (blue) and ML Y-Bi2212 (left to
 13 the pink dashed line, as indicated by the arrow). The three probing spots are marked by black
 14 (suspended ML covered by hBN), red (SiO₂ supported area covered by hBN), and green
 15 (uncovered supported area) dots. The scale bar is 5 μm. (c) Pump-probe responses at 1.6 K for
 16 the ML sample, corresponding to the three dots in (b). Superconductivity is only preserved in the
 17 hBN covered supported area.

1
2
3
4
5
6
7
8
9
10
11
12
13
14
15
16

To summarize, we have studied the superconducting phase transition in high-quality Y-Bi2212 samples of atomic thickness using an optical pump-probe technique. The optical approach provides a noninvasive way to probe the superconductivity with a micrometer spatial resolution and to identify the intrinsic T_c , which is close to the bulk limit. We find that the decay time constant shows a divergent-like behavior near T_c , and observe a pump-induced phase transition at high fluence, consistent with previous reports for bulk samples. These findings indicate that superconductivity persists in Bi2212 with reduced dimension, confirming the 2D nature of the electronic correlations of the superconducting condensate. Furthermore, we uncover significant effects of the local environment and flake thickness on the pump-probe response of atomically thin samples. We spatially resolve the pump-probe signals of different signs and amplitudes, which can be attributed to different optical excitations in different local dielectric environments. Remarkably, we find that the superconductivity in the monolayer sample is extraordinarily sensitive to exposed surfaces, which highlights the importance of protective encapsulation layers. Our understanding of optical properties of atomically thin cuprates may pave the way for their potential applications in optoelectronics and photon-based quantum computing^{44,45}.

17
18
19

ASSOCIATED CONTENT

20 **Supporting information**

21 The following files are available free of charge:

22 Supporting Information: Detailed experimental methods, temperature dependence analysis, and
23 the additional transport experiment (PDF)

1 **AUTHOR INFORMATION**

2 **Corresponding author**

3 *Ziliang Ye, E-mail: zlye@phas.ubc.ca

4 **Author contributions**

5 # These authors contribute equally to this paper. Z.Y. conceived the idea and managed the
6 project. Y.X. fabricated the samples with the assistance from D.Y., J.L., and K.A.. Y.X., J.W.
7 and J.D. built the setup and performed the measurements. M.Z., M.B., A.D., H.E., M.G., K.W.,
8 and T.T. provided the bulk crystals. Y.X. and Z.Y. performed the analysis and wrote the
9 manuscript with input from all other authors.

10 **Notes**

11 The authors declare that they have no conflict of interest.

12 **ACKNOWLEDGEMENTS**

13 We acknowledge the fruitful discussions with Frank Zhao and Hsiang-Hsi Kung, as well as the
14 technical support from Giorgio Levy and Vinit Doke. This research was undertaken thanks in
15 part to funding from the Max Planck-UBC-UTokyo Center for Quantum Materials and the
16 Canada First Research Excellence Fund, Quantum Materials and Future Technologies Program
17 and Gordon and Betty Moore Foundation's EPiQS Initiative (GBMF11071). The work at the
18 University of Minnesota was funded by the U.S. Department of Energy through the University of
19 Minnesota Center for Quantum Materials, under Grant No. DE-SC0016371. This project was
20 also funded by the Natural Sciences and Engineering Research Council of Canada (NSERC); the
21 Canada Foundation for Innovation (CFI); the Department of National Defence (DND); the
22 British Columbia Knowledge Development Fund (BCKDF); the Canada Research Chairs
23 Program (Z.Y., A.D.); and the CIFAR Quantum Materials Program (A.D.).

24

25

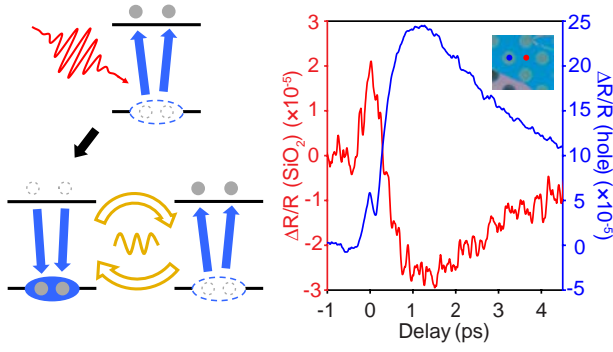
1 REFERENCES

- 2 (1) Yu, Y.; Ma, L.; Cai, P.; Zhong, R.; Ye, C.; Shen, J.; Gu, G. D.; Chen, X. H.; Zhang, Y.
3 High-Temperature Superconductivity in Monolayer $\text{Bi}_2\text{Sr}_2\text{CaCu}_2\text{O}_{8+\delta}$. *Nature* **2019**, *575*
4 (7781), 156–163.
- 5 (2) Zhao, S. Y. F.; Cui, X.; Volkov, P. A.; Yoo, H.; Lee, S.; Gardener, J. A.; Akey, A. J.;
6 Engelke, R.; Ronen, Y.; Zhong, R.; Gu, G.; Plugge, S.; Tummuru, T.; Kim, M.; Franz, M.;
7 Pixley, J. H.; Poccia, N.; Kim, P. Time-Reversal Symmetry Breaking Superconductivity
8 between Twisted Cuprate Superconductors. *Science* **2023**, *382* (6677), 1422–1427.
- 9 (3) Zhu, Y.; Liao, M.; Zhang, Q.; Xie, H.-Y.; Meng, F.; Liu, Y.; Bai, Z.; Ji, S.; Zhang, J.; Jiang,
10 K.; Zhong, R.; Schneeloch, J.; Gu, G.; Gu, L.; Ma, X.; Zhang, D.; Xue, Q.-K. Presence of s -
11 Wave Pairing in Josephson Junctions Made of Twisted Ultrathin $\text{Bi}_2\text{Sr}_2\text{CaCu}_2\text{O}_{8+x}$ Flakes.
12 *Phys. Rev. X* **2021**, *11* (3), 031011.
- 13 (4) Ghosh, S.; Patil, V.; Basu, A.; Kuldeep; Dutta, A.; Jangade, D. A.; Kulkarni, R.;
14 Thamizhavel, A.; Steiner, J. F.; von Oppen, F.; Deshmukh, M. M. *High-Temperature*
15 *Josephson Diode*. arXiv.org. <https://doi.org/10.48550/arXiv.2210.11256>
- 16 (5) Zhu, Y.; Wang, H.; Wang, Z.; Hu, S.; Gu, G.; Zhu, J.; Zhang, D.; Xue, Q.-K. Persistent
17 Josephson Tunneling between $\text{Bi}_2\text{Sr}_2\text{CaCu}_2\text{O}_{8+x}$ Flakes Twisted by 45° across the
18 Superconducting Dome. *Phys. Rev. B* **2023**, *108* (17), 174508.
- 19 (6) Can, O.; Tummuru, T.; Day, R. P.; Elfimov, I.; Damascelli, A.; Franz, M. High-
20 Temperature Topological Superconductivity in Twisted Double-Layer Copper Oxides. *Nat.*
21 *Phys.* **2021**, *17* (4), 519–524.
- 22 (7) Volkov, P. A.; Wilson, J. H.; Lucht, K. P.; Pixley, J. H. Current- and Field-Induced
23 Topology in Twisted Nodal Superconductors. *Phys. Rev. Lett.* **2023**, *130* (18), 186001.
- 24 (8) Volkov, P. A.; Wilson, J. H.; Lucht, K. P.; Pixley, J. H. Magic Angles and Correlations in
25 Twisted Nodal Superconductors. *Phys. Rev. B* **2023**, *107* (17), 174506.
- 26 (9) Jiang, D.; Hu, T.; You, L.; Li, Q.; Li, A.; Wang, H.; Mu, G.; Chen, Z.; Zhang, H.; Yu, G.;
27 Zhu, J.; Sun, Q.; Lin, C.; Xiao, H.; Xie, X.; Jiang, M. High- T_c Superconductivity in
28 Ultrathin $\text{Bi}_2\text{Sr}_2\text{CaCu}_2\text{O}_{8+x}$ down to Half-Unit-Cell Thickness by Protection with Graphene.
29 *Nat. Commun.* **2014**, *5* (1), 5708.
- 30 (10) Zhao, S. Y. F.; Poccia, N.; Panetta, M. G.; Yu, C.; Johnson, J. W.; Yoo, H.; Zhong, R.; Gu,
31 G. D.; Watanabe, K.; Taniguchi, T.; Postolova, S. V.; Vinokur, V. M.; Kim, P. Sign-
32 Reversing Hall Effect in Atomically Thin High-Temperature $\text{Bi}_{2.1}\text{Sr}_{1.9}\text{CaCu}_2\text{O}_{8+\delta}$
33 Superconductors. *Phys. Rev. Lett.* **2019**, *122* (24), 247001.
- 34 (11) Liao, M.; Zhu, Y.; Zhang, J.; Zhong, R.; Schneeloch, J.; Gu, G.; Jiang, K.; Zhang, D.; Ma,
35 X.; Xue, Q.-K. Superconductor–Insulator Transitions in Exfoliated $\text{Bi}_2\text{Sr}_2\text{CaCu}_2\text{O}_{8+\delta}$ Flakes.
36 *Nano Lett.* **2018**, *18* (9), 5660–5665.
- 37 (12) Sterpetti, E.; Biscaras, J.; Erb, A.; Shukla, A. Comprehensive Phase Diagram of Two-
38 Dimensional Space Charge Doped $\text{Bi}_2\text{Sr}_2\text{CaCu}_2\text{O}_{8+x}$. *Nat. Commun.* **2017**, *8* (1), 2060.
- 39 (13) Giannetti, C.; Capone, M.; Fausti, D.; Fabrizio, M.; Parmigiani, F.; Mihailovic, D. Ultrafast
40 Optical Spectroscopy of Strongly Correlated Materials and High-Temperature
41 Superconductors: A Non-Equilibrium Approach. *Advances in Physics* **2016**, *65* (2), 58–238.
- 42 (14) Rothwarf, A.; Taylor, B. N. Measurement of Recombination Lifetimes in Superconductors.
43 *Phys. Rev. Lett.* **1967**, *19* (1), 27–30.
- 44 (15) Kabanov, V. V.; Demsar, J.; Mihailovic, D. Kinetics of a Superconductor Excited with a
45 Femtosecond Optical Pulse. *Phys. Rev. Lett.* **2005**, *95* (14), 147002.

- 1 (16) Kabanov, V. V.; Demsar, J.; Podobnik, B.; Mihailovic, D. Quasiparticle Relaxation
2 Dynamics in Superconductors with Different Gap Structures: Theory and Experiments on
3 $\text{YBa}_2\text{Cu}_3\text{O}_{7-\delta}$. *Phys. Rev. B* **1999**, *59* (2), 1497–1506.
- 4 (17) Liu, Y. H.; Toda, Y.; Shimatake, K.; Momono, N.; Oda, M.; Ido, M. Direct Observation of
5 the Coexistence of the Pseudogap and Superconducting Quasiparticles in $\text{Bi}_2\text{Sr}_2\text{CaCu}_2\text{O}_{8+y}$
6 by Time-Resolved Optical Spectroscopy. *Phys. Rev. Lett.* **2008**, *101* (13), 137003.
- 7 (18) Toda, Y.; Mertelj, T.; Kusar, P.; Kurosawa, T.; Oda, M.; Ido, M.; Mihailovic, D.
8 Quasiparticle Relaxation Dynamics in Underdoped $\text{Bi}_2\text{Sr}_2\text{CaCu}_2\text{O}_{8+\delta}$ by Two-Color Pump-
9 Probe Spectroscopy. *Phys. Rev. B* **2011**, *84* (17), 174516.
- 10 (19) Gedik, N.; Blake, P.; Spitzer, R. C.; Orenstein, J.; Liang, R.; Bonn, D. A.; Hardy, W. N.
11 Single-Quasiparticle Stability and Quasiparticle-Pair Decay in $\text{YBa}_2\text{Cu}_3\text{O}_{6.5}$. *Phys. Rev. B*
12 **2004**, *70* (1), 014504.
- 13 (20) Graf, J.; Jozwiak, C.; Smallwood, C. L.; Eisaki, H.; Kaindl, R. A.; Lee, D.-H.; Lanzara, A.
14 Nodal Quasiparticle Meltdown in Ultrahigh-Resolution Pump-Probe Angle-Resolved
15 Photoemission. *Nat. Phys.* **2011**, *7* (10), 805–809.
- 16 (21) Cortés, R.; Rettig, L.; Yoshida, Y.; Eisaki, H.; Wolf, M.; Bovensiepen, U. Momentum-
17 Resolved Ultrafast Electron Dynamics in Superconducting $\text{Bi}_2\text{Sr}_2\text{CaCu}_2\text{O}_{8+\delta}$. *Phys. Rev.*
18 *Lett.* **2011**, *107* (9), 097002.
- 19 (22) Lee, P. A.; Nagaosa, N.; Wen, X.-G. Doping a Mott Insulator: Physics of High-
20 Temperature Superconductivity. *Rev. Mod. Phys.* **2006**, *78* (1), 17–85.
- 21 (23) Scalapino, D. J. A Common Thread: The Pairing Interaction for Unconventional
22 Superconductors. *Rev. Mod. Phys.* **2012**, *84* (4), 1383–1417.
- 23 (24) Fradkin, E.; Kivelson, S. A.; Tranquada, J. M. Colloquium: Theory of Intertwined Orders in
24 High Temperature Superconductors. *Rev. Mod. Phys.* **2015**, *87* (2), 457–482.
- 25 (25) Boschini, F.; da Silva Neto, E. H.; Razzoli, E.; Zonno, M.; Peli, S.; Day, R. P.; Michiardi,
26 M.; Schneider, M.; Zwartsenberg, B.; Nigge, P.; Zhong, R. D.; Schneeloch, J.; Gu, G. D.;
27 Zhdanovich, S.; Mills, A. K.; Levy, G.; Jones, D. J.; Giannetti, C.; Damascelli, A. Collapse
28 of Superconductivity in Cuprates via Ultrafast Quenching of Phase Coherence. *Nat. Mater.*
29 **2018**, *17* (5), 416–420.
- 30 (26) Emery, V. J.; Kivelson, S. A. Importance of Phase Fluctuations in Superconductors with
31 Small Superfluid Density. *Nature* **1995**, *374* (6521), 434–437.
- 32 (27) Bollinger, A. T.; Božović, I. Two-Dimensional Superconductivity in the Cuprates Revealed
33 by Atomic-Layer-by-Layer Molecular Beam Epitaxy. *Supercond. Sci. Technol.* **2016**, *29*
34 (10), 103001.
- 35 (28) Li, Q.; Hücker, M.; Gu, G. D.; Tsvelik, A. M.; Tranquada, J. M. Two-Dimensional
36 Superconducting Fluctuations in Stripe-Ordered $\text{La}_{1.875}\text{Ba}_{0.125}\text{CuO}_4$. *Phys. Rev. Lett.* **2007**,
37 *99* (6), 067001.
- 38 (29) Pan, S. H.; Hudson, E. W.; Ma, J.; Davis, J. C. Imaging and Identification of Atomic Planes
39 of Cleaved $\text{Bi}_2\text{Sr}_2\text{CaCu}_2\text{O}_{8+\delta}$ by High Resolution Scanning Tunneling Microscopy. *Appl.*
40 *Phys. Lett.* **1998**, *73* (1), 58–60.
- 41 (30) Coslovich, G.; Giannetti, C.; Cilento, F.; Dal Conte, S.; Ferrini, G.; Galinetto, P.; Greven,
42 M.; Eisaki, H.; Raichle, M.; Liang, R.; Damascelli, A.; Parmigiani, F. Evidence for a
43 Photoinduced Nonthermal Superconducting-to-Normal-State Phase Transition in
44 Overdoped $\text{Bi}_2\text{Sr}_2\text{Ca}_{0.92}\text{Y}_{0.08}\text{Cu}_2\text{O}_{8+\delta}$. *Phys. Rev. B* **2011**, *83* (6), 064519.
- 45 (31) Schuller, I.; Gray, K. E. Experimental Observation of the Relaxation Time of the Order
46 Parameter in Superconductors. *Phys. Rev. Lett.* **1976**, *36* (8), 429–432.

- 1 (32) Han, S. G.; Vardeny, Z. V.; Wong, K. S.; Symko, O. G.; Koren, G. Femtosecond Optical
2 Detection of Quasiparticle Dynamics in High- T_c $\text{YBa}_2\text{Cu}_3\text{O}_{7-\delta}$ Superconducting Thin Films.
3 *Phys. Rev. Lett.* **1990**, *65* (21), 2708–2711.
- 4 (33) Kusar, P.; Kabanov, V. V.; Demsar, J.; Mertelj, T.; Sugai, S.; Mihailovic, D. Controlled
5 Vaporization of the Superconducting Condensate in Cuprate Superconductors by
6 Femtosecond Photoexcitation. *Phys. Rev. Lett.* **2008**, *101* (22), 227001.
- 7 (34) Giannetti, C.; Coslovich, G.; Cilento, F.; Ferrini, G.; Eisaki, H.; Kaneko, N.; Greven, M.;
8 Parmigiani, F. Discontinuity of the Ultrafast Electronic Response of Underdoped
9 Superconducting $\text{Bi}_2\text{Sr}_2\text{CaCu}_2\text{O}_{8+\delta}$ Strongly Excited by Ultrashort Light Pulses. *Phys. Rev.*
10 *B* **2009**, *79* (22), 224502.
- 11 (35) Kaindl, R. A.; Carnahan, M. A.; Chemla, D. S.; Oh, S.; Eckstein, J. N. Dynamics of Cooper
12 Pair Formation in $\text{Bi}_2\text{Sr}_2\text{CaCu}_2\text{O}_{8+\delta}$. *Phys. Rev. B* **2005**, *72* (6), 060510.
- 13 (36) Averitt, R. D.; Rodriguez, G.; Lobad, A. I.; Siders, J. L. W.; Trugman, S. A.; Taylor, A. J.
14 Nonequilibrium Superconductivity and Quasiparticle Dynamics in $\text{YBa}_2\text{Cu}_3\text{O}_{7-\delta}$. *Phys. Rev.*
15 *B* **2001**, *63* (14), 140502.
- 16 (37) Pelc, D.; Vučković, M.; Grbić, M. S.; Požek, M.; Yu, G.; Sasagawa, T.; Greven, M.; Barišić,
17 N. Emergence of Superconductivity in the Cuprates via a Universal Percolation Process.
18 *Nat. Commun.* **2018**, *9* (1), 4327.
- 19 (38) Popčević, P.; Pelc, D.; Tang, Y.; Velebit, K.; Anderson, Z.; Nagarajan, V.; Yu, G.; Požek,
20 M.; Barišić, N.; Greven, M. Percolative Nature of the Direct-Current Paraconductivity in
21 Cuprate Superconductors. *npj Quant. Mater.* **2018**, *3* (1), 1–6.
- 22 (39) Pelc, D.; Anderson, Z.; Yu, B.; Leighton, C.; Greven, M. Universal Superconducting
23 Precursor in Three Classes of Unconventional Superconductors. *Nat. Commun.* **2019**, *10* (1),
24 2729.
- 25 (40) Segre, G. P.; Gedik, N.; Orenstein, J.; Bonn, D. A.; Liang, R.; Hardy, W. N. Photoinduced
26 Changes of Reflectivity in Single Crystals of $\text{YBa}_2\text{Cu}_3\text{O}_{6.5}$ (Ortho II). *Phys. Rev. Lett.* **2002**,
27 *88* (13), 137001.
- 28 (41) Giannetti, C.; Cilento, F.; Conte, S. D.; Coslovich, G.; Ferrini, G.; Molegraaf, H.; Raichle,
29 M.; Liang, R.; Eisaki, H.; Greven, M.; Damascelli, A.; van der Marel, D.; Parmigiani, F.
30 Revealing the High-Energy Electronic Excitations Underlying the Onset of High-
31 Temperature Superconductivity in Cuprates. *Nat. Commun.* **2011**, *2* (1), 353.
- 32 (42) Stojchevska, L.; Kusar, P.; Mertelj, T.; Kabanov, V. V.; Toda, Y.; Yao, X.; Mihailovic, D.
33 Mechanisms of Nonthermal Destruction of the Superconducting State and Melting of the
34 Charge-Density-Wave State by Femtosecond Laser Pulses. *Phys. Rev. B* **2011**, *84* (18),
35 180507.
- 36 (43) Gedik, N.; Langner, M.; Orenstein, J.; Ono, S.; Abe, Y.; Ando, Y. Abrupt Transition in
37 Quasiparticle Dynamics at Optimal Doping in a Cuprate Superconductor System. *Phys. Rev.*
38 *Lett.* **2005**, *95* (11), 117005.
- 39 (44) Charaev, I.; Bandurin, D. A.; Bollinger, A. T.; Phinney, I. Y.; Drozdov, I.; Colangelo, M.;
40 Butters, B. A.; Taniguchi, T.; Watanabe, K.; He, X.; Medeiros, O.; Božović, I.; Jarillo-
41 Herrero, P.; Berggren, K. K. Single-Photon Detection Using High-Temperature
42 Superconductors. *Nat. Nanotechnol.* **2023**, *18* (4), 343–349.
- 43 (45) Merino, R. L.; Seifert, P.; Retamal, J. D.; Mech, R. K.; Taniguchi, T.; Watanabe, K.;
44 Kadowaki, K.; Hadfield, R. H.; Efetov, D. K. Two-Dimensional Cuprate Nanodetector with
45 Single Telecom Photon Sensitivity at $T = 20$ K. *2D Mater.* **2023**, *10* (2), 021001.
- 46

1 TOC Graphic



2